NANOSYSTEMS:
PHYSICS, CHEMISTRY, MATHEMATICS

Original article

Lobinsky A.A., et al. *Nanosystems: Phys. Chem. Math.*, 2023, **14** (5), 554–559.
http://nanojournal.ifmo.ru
DOI 10.17586/2220-8054-2023-14-5-554-559

SILD synthesis of porous manganese oxide nanocoatings as electroactive materials for pseudocapacitors

Artem A. Lobinsky, Maria V. Kaneva, Anastasia K. Bachina, Maxim I. Tenevich

Ioffe Institute, St. Petersburg, Russia

Corresponding author: Artem A. Lobinsky, lobinski.a@mail.ru

PACS 81.07.Bc

ABSTRACT In present work the porous nanocoating of manganese oxide were obtained via successive ionic layer deposition from aqueous solutions of potassium permanganate and DMSO. The morphology, phase and chemical composition of the synthesized nanocoatings were characterized by XRD, SEM, EDX and Raman spectroscopy. The possibility of controlled changes in the morphology of the resulting compounds was demonstrated by changing the concentration of reagents and the number of processing cycles in order to obtain optimal electrochemical characteristics. Electrodes based on nickel foam and coated with films of porous manganese oxide showed high specific capacity (1324 and 297 F/g at a current density of 1 A/g in 1 M NaOH and 1 M Na_2SO_4, respectively), both in neutral and in aqueous alkaline electrolytes.

KEYWORDS manganese oxide, SILD, nanocoatings, electrode materials, pseudocapacitor

ACKNOWLEDGEMENTS This research was financial supported by grant of the President of the Russian Federation for state support of young Russian scientists (grant number MK-3864.2022.1.3). The SEM and PXRD study was conducted utilizing equipment at the Engineering Center of the St. Petersburg State Institute of Technology. The authors gratefully acknowledge to the Center for Optical and Laser Materials Research of St. Petersburg State University.

FOR CITATION Lobinsky A.A., Kaneva M.V., Bachina A.K., Tenevich M.I. SILD synthesis of porous manganese oxide nanocoatings as electroactive materials for pseudocapacitors. *Nanosystems: Phys. Chem. Math.*, 2023, **14** (5), 554–559.

1. Introduction

The increasing demand for more energy every year and the growing environmental problems caused by the burning of limited reserves of fossil fuels encourage the search and use of new, highly efficient and environmentally friendly energy sources [1, 2].

Supercapacitors (SCs) are promising energy storage devices that are characterized by large capacity relative to size, extremely low level of series resistance and high charging speed, which makes them very promising for use in power grids, electric vehicles and portable equipment [3, 4]. Of particular interest are the so-called pseudocapacitors (PSCs), in which energy is stored at the cathode in a double electric layer, and at the anode due to the flow of Faraday processes. Thus, they combine the advantages of electrochemical double-layer (ECDL) supercapacitors (charge rate and cyclic stability) and metal-ion batteries (high energy density), which makes their further application promising [5].

Among the electrode materials for cathodes and anodes of ECDL SCs, carbon materials are most often used, but they have low specific capacity and energy values. The most effective cathode material for PSCs turned out to be ruthenium oxide, since it has high values of theoretical specific capacitance due to the manifestation of the pseudocapacitance, but at the same time such a material is quite expensive, which limits commercial use [6].

Manganese oxides, in particular MnO_2, are effective electrode materials for chemical current sources because they have a high theoretical specific capacity (1370 F/g) and cycling stability, as well as good stability in various environments [7–9]. However, the obtained specific capacitances of pure MnO_2 are much lower than the theoretical capacity, which is likely due to the low active surface area, poor conductivity, as well as low ion diffusion. Among many ways to increase the capacitive characteristics of the MnO_2 electrode material, increasing its specific surface area by adjusting the pore size and size distribution is considered promising, which can provide better interfacial contact between the electrode and the electrolyte [10]. Thus, the development of methods for the selective synthesis of manganese oxide is a key task for obtaining highly efficient electrode materials.

Currently, several routes are used for the synthesis of manganese oxide nanocoating, namely, hydrothermal route [11], sol-gel route [12], redox reaction [13], thermal decomposition [14], refluxing route [15], co-precipitation [16], etc. However, the presented methods for the synthesis of manganese oxide have a number of limitations related to the duration of the process, the use of devices with high temperature and pressure, higher synthesis temperatures, as well as limiting of the number of possible substrates.

© Lobinsky A.A., Kaneva M.V., Bachina A.K., Tenevich M.I., 2023

In this research, we propose a novel controllable reduction route synthesis of nanocoatings of manganese oxide on nickel foam via successive ionic layer deposition (SILD) [17,18] technique from aqueous solutions of manganese permanganate and dimethyl sulfoxide (DMSO) and investigation its application as effective electrode materials for pseudocapacitor in neutral and alkaline electrolytes. The proposed synthesis route is based on the reduction of $KMnO_4$ in an aqueous solution of DMSO with different concentrations. The reduction of potassium permanganate by organic compounds is a common method for obtaining manganese oxides [19], however, as far as we know, this route has not been previously used in the SILD method. The production of nanocoats in this way has the advantages of being able to obtain ultrathin oxide films on the surface of various substrates under conditions of "soft chemistry". Previously, the SILD method has already been successfully used by us to obtain nanocoatings of transition metal oxides and hydroxides [20–22], in particular manganese oxide [23–25].

2. Experimental

2.1. Fabrication of MnO_2/nickel foam electrode

Nickel foam (NF) plates (110 PPI, surface area 1 cm^2) were used as substrates. The synthesis of manganese oxide nanocoating was carried out using the SILD method with the occurrence of a reduction reaction on the surface of the nickel foam substrate. As the first reagent for synthesis aqueous solutions of $KMnO_4$ (0.01 M) salt were used, and as a second reagent aqueous solution of DMSO (99, 75, 50 and 25 %) is used. The substrates were processed by successive immersion in reagent solutions according to a certain scheme forming one SILD cycle. First, the substrate was immersed in the solution of the first reagent for 30 seconds, then it was washed off the excess reagent in distilled water for 15 seconds. Then the substrate was immersed in a solution of the second reagent and washed again with distilled water for the same time, respectively. As a result of the reduction reaction of MnO_4^{+7} to Mn^{+4} in DMSO, a layer of sparingly soluble manganese oxide nanocoating on nickel foam surface was formed. After synthesis, the electrodes were dried in air for 24 hours.

The number of SILD cycles was chosen in such a way that it allows on to ensure optimal layer thickness and, at the same time, sufficient mass (1 – 2 mg) required for electrochemical measurements. Concentrations of the DMSO were selected on the basis of preliminary experiments, during which their electrochemical characteristics were analyzed. The 30 SILD cycles and a DMSO concentration of 25 % were chosen as optimal.

2.2. Materials characterization

The morphology and chemical composition of synthesized nanocoating were examined by scanning electron microscopy (SEM) (Tescan Vega 3 SBH microscope) and energy-dispersive X-ray spectroscopy (EDX) (Oxford INCA x-act X-ray) technique. Powder X-ray diffraction (PXRD) patterns were acquired using a Rigaku SmartLab 3 X-ray diffractometer, equipped with a Dtex silicon 1-D detector. The X-ray source employed Cu Kα radiation with a wavelength (λ) of 1.540593 Å, operating at a voltage of 50 kV and a current of 40 mA. These measurements were carried out utilizing a zero-background silicon holder. The phase identification was accomplished through the utilization of the powder standard database ICSD. Raman spectroscopy measurement was performed with a SENTERRA (Bruker) spectrometer with 633 nm wavelength laser excitation.

2.3. Electrochemical measurement

The electrochemical characteristics of synthesized nanolayers as electrode material for pseudocapacitors were studied used cyclic voltammetry (CVA) and galvanostatic charge-discharge (GCD) techniques using Elins P45-X potentiostat/galvanostat. The fabricated working electrodes were measured in a three-electrode electrochemical cell. The Ag/AgCl electrode (neutral media) or Hg/HgO electrode (alkaline media) was used as an reference electrode and the graphite rod was used as an counter electrode. All measurements were carried out at room temperature and atmospheric pressure in aqueous solutions of 1 M Na_2SO_4 or 1 M NaOH, which were used as an electrolyte.

3. Result and discussion

The PXRD pattern obtained for the synthesized sample exhibits diffuse features with broad, low-intensity peaks, as depicted in Fig. 1(a). Phase analysis revealed that the structure of the sample corresponds to the turbostatic birnessite-type. However, differentiating between monoclinic (Space Group: C12/m1) and hexagonal (Space Group: P63/mmc) symmetry is challenging due to the pure crystallinity of the sample. The prominent characteristic reflexes associated with the birnessite structure are highlighted in Fig. 1(b). The shape of the XRD pattern suggests a small crystallite size, imperfections, and the turbostatic nature of the sample. The extinction of some reflexes in the pattern provides evidence for morphological anisotropy observed in such morphological objects like plate-like, lamellar, sheet-like ones.

Birnessite phases are characterized by a layered structure composed of single sheets of [MnO_6] octahedrons [26]. In natural birnessite, water molecules and alkaline metal ions are known to occupy the interlayer spaces between the octahedral layers of [MnO_6], typically resulting in a distance between layers of approximately 7 Å [26, 27]. However, in synthetic birnessite, interlayer spaces are predominantly occupied by H_2O molecules, leading to an increased distance

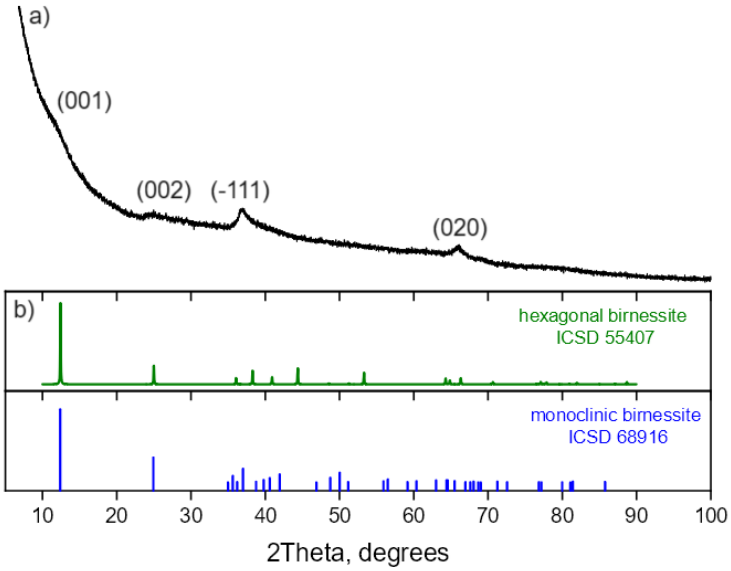

FIG. 1. PXRD pattern of the MnO_2 nanocoatings obtained by SILD method (a) and patterns of the references from ICSD (b)

between successive layers of manganese octahedrons. In turbostatic structures, order within the planes in the *a* and *b* directions is maintained, but there can be a misalignment or complete disorientation within the plane in the *c* direction [28]. The most intense peak at around $2\theta = 12\ ^\circ$ in the PXRD pattern (Fig. 1(a)) is the indicator of the order in the *c* direction. However, this peak is weak, suggesting a severe misalignment between manganese octahedron layers. The location of this peak corresponds to a d-spacing of 7.38 [$\pm$10] Å.

The analysis of SEM data confirms the porous morphology of the synthesized sample. As shown in Fig. 2(a) nanocoating is formed by spherical-like micron-size aggregates of randomly shaped structures. SEM image with higher magnification (Fig. 2(b)), shows that the structure of MnO_2 is porous and built up of set nanosheets with flower-like morphology. EDX results indicate the presence of Mn and O atoms with a small impurity of C, K and S atoms in the nanocoating (no more than 1 %).

The Raman spectrum, presented in Fig. 3, supports the hexagonal birnessite-type structure of the synthesized sample. The relationship between the two highest frequency modes (at around 570 and 680 cm^{-1}) is characteristic of the hexagonal birnessite-type structure 4. Moreover, the shift of the high frequency mode at 680 cm^{-1} aroused from [MnO_6] octahedral layer's motions parallel to layer stacking direction is dependent on the interlayer spacing in birnessite-type structures [29, 30]. In work [30], a plot was constructed, depicting the relationship between the Raman shift of the high-frequency mode and the d-spacing, which was subsequently linearly approximated. The determined d-spacing value of 7.38 [$\pm$10] Å and the observed shift of the high-frequency mode to 680 cm^{-1}, as determined in the present study, closely align with the

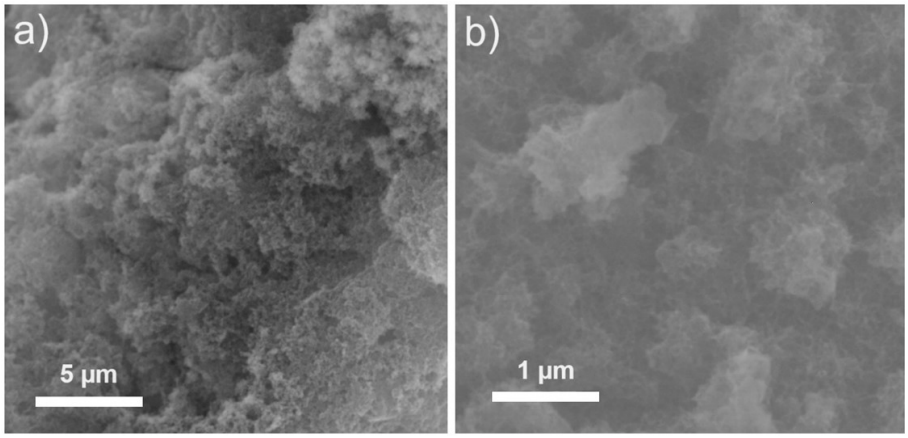

FIG. 2. SEM images of manganese oxide nanocoatings obtained after 30 treatment SILD cycles at lower (a) and at a higher magnification (b)

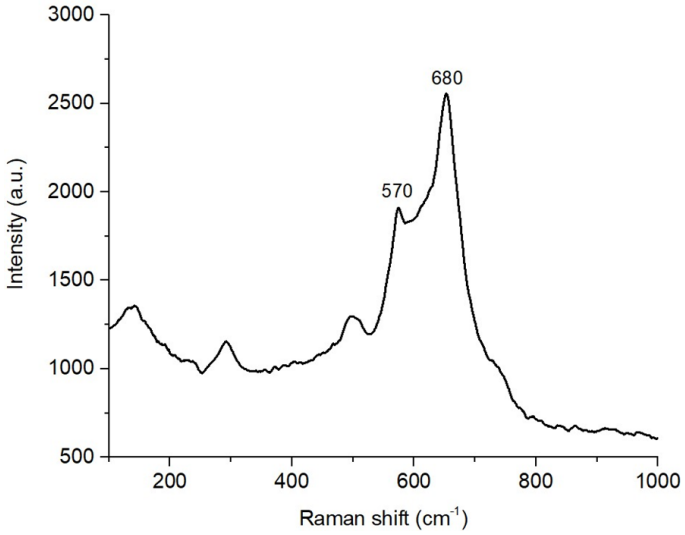

FIG. 3. Raman spectrum of the MnO_2 nanocoatings obtained by SILD method

results of this approximation. The observed consistency, coupled with an analysis of the intensity distribution of high-frequency modes, serves as additional confirmation of the presence of a hexagonal birnessite-type structure within the obtained sample, characterized by the exclusive intercalation of water molecules between the octahedral layers.

Further, the electrochemical characteristics of the obtained nanocoatings as pseudocapacitor electrodes were evaluated. In an alkaline electrolyte (1 M NaOH) in the electroactive layer of MnO_2, the Mn(IV)/Mn(III) redox reaction occurred, which was observed through wide cathode and anode peaks on the CVA curve Fig. 4(a). In a neutral electrolyte (1 M Na_2SO_4), MnO_2 electrodes demonstrated pseudocapacitance behavior. The shape of the CVA was close to rectangular with small peaks on the cathode and anode curves Fig. 4(c). The anodic peak is observed at 0.70 V, and the cathodic peak at 0.55 V. This redox process may reflect the redox transitions of the manganese Mn(IV)/Mn(III) or can be related to the cation intercalatioin/deintercalation.

The specific capacitance was determined from the galvanostatic charge-discharge curves shown in Fig. 4(b,d) for an alkaline and neutral medium, respectively. The measurement was performed at a current density of 1 A/g. The shape of the charge-discharge curves, as well as the CVA, was typical for pseudocapacitors.

Specific capacities for alkaline and neutral media were 1324 and 297 F/g at current density 1 A/g, respectively. The obtained high specific capacitances can be explained by the unique porous thin-film structure of MnO_2-based electrodes. The developed morphology and turbostatic structure provides a large number of active sites and a high specific surface area, which ultimately provides excellent capacitive characteristics.

4. Conclusion

For the first time, manganese oxide of the hexagonal turbostatic birnessite-type was successfully synthesized by a direct and simple route based on the reduction of $KMnO_4$ by DMSO via SILD method. The characterization of the nanocoating showed that MnO_2 synthesized in this way has a layered structure with an interlayer space of 7.38 Å and nanoscale crystallites. The morphology obtained by the SEM method, which showed that the nanocoating has a porous structure formed by a set of nanosheets. At the final stage of the study, the electrochemical characteristics of electrodes based on nickel foam with manganese oxide nanocoating were studied. The electrodes demonstrated pseudo-capacitive behaviour and high specific capacitance in both alkaline and neutral electrolytes. Thus, it was shown that the proposed route for the synthesis of MnO_2 makes it possible to obtain a highly efficient capacitive material in conditions of “soft chemistry” without the use of complex and expensive equipment.

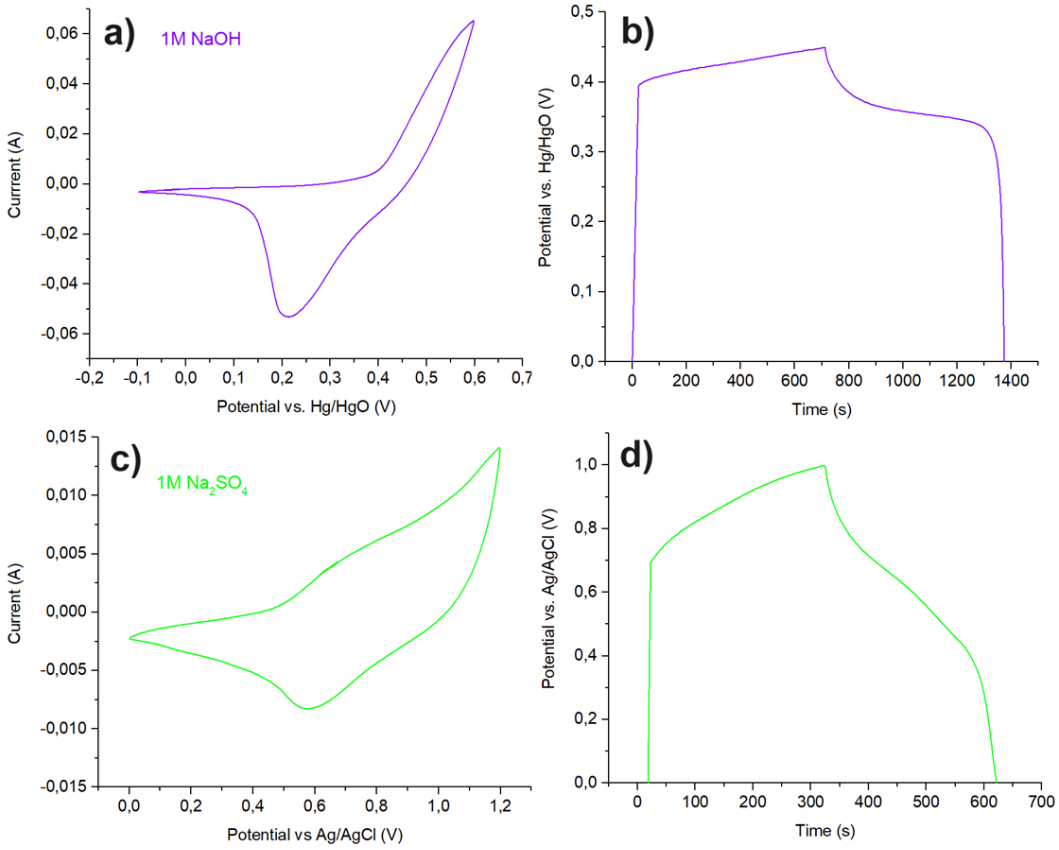

FIG. 4. CVA curves of MnO_2/NF at scan rate 10 mV/s in 1 M NaOH (a) and 1 M Na_2SO_4 (c). Galvanostatic charge–discharge curves of MnO_2/NF at current density 1 A/g in 1 M NaOH (b) and 1 M Na_2SO_4 (d)

References

[1] Liu C., Li F., Ma L.-P., Cheng H.-M. Advanced Materials for Energy Storage. *Adv. Mater.*, 2010, **22**, P. 28–62.

[2] Zhou G., Li F., Cheng H.-M. Progress in flexible lithium batteries and future prospects. *Energy Environ. Sci.*, 2014, **7**, P. 1307–1338.

[3] Wang G., Zhang L., Zhang J. A review of electrode materials for electrochemical supercapacitors. *Chem. Soc. Rev.*, 2012, **41**, P. 797–828.

[4] Zhong C., Deng Y., Hu W., Qiao J., Zhang L., Zhang J. A review of electrolyte materials and compositions for electrochemical supercapacitors. *Chem. Soc. Rev.*, 2015, **44**, P. 7484–7539.

[5] Bhojane P. Recent advances and fundamentals of Pseudocapacitors: Materials, mechanism, and its understanding. *J. Energy Storage*, 2022, **45**, 103654.

[6] Sahin M., Blaabjerg F., Sangwongwanich A. A Comprehensive Review on Supercapacitor Applications and Developments. *Energies (Basel)*, 2022, **15** (3), P. 674–699.

[7] Wei W., Cui X., Chen W., Ivey D.G. Manganese oxide-based materials as electrochemical supercapacitor electrodes. *Chem. Soc. Rev.*, 2011, **40**, P. 1697–1721.

[8] Simin He, Zunli Mo, Chao Shuai, Wentong Liu, Ruimei Yue, Guigui Liu, Hebing Pei, Ying Chen, Nijuan Liu, Ruibin Guo. Pre-intercalation δ-MnO_2 zinc-ion hybrid supercapacitor with high energy storage and ultra-long cycle life. *Applied Surface Science*, 2022, **577**, 151904.

[9] Gao Y.N., Yang H.Y., Bai Y., Wu C. Mn-based oxides for aqueous rechargeable metal ion batteries. *J. Mater. Chem. A*, 2021, **9**, P.11472–11500.

[10] Julien C., Mauger A. Nanostructured MnO_2 as electrode materials for energy storage. *Nanomaterials*, 2017, **7**, 396.

[11] Subramanian V., Zhu H., Vajtai R., Ajayan P.M., Wei B. Hydrothermal synthesis and pseudocapacitance properties of MnO_2 nanostructures. *J. Phys. Chem. B*, 2005, **109**, P. 20207–20214.

[12] Hashem A.M., Abdel-Ghany A.E., El-Tawil R., Bhaskar A., Hunzinger B., Ehrenberg H., Mauger A., Julien C.M. Urchin-like α-MnO_2 formed of nano-needles for high-performance lithium batteries. *Ionics*, 2016, **22**, P. 2263–2271.

[13] Yin B., Zhang S., Jiang H., Qu F., Wu X. Phase-controlled synthesis of polymorphic MnO_2 structures for electrochemical energy storage. *J. Mater. Chem.*, 2015, **3**, P. 5722–5729.

[14] Alfaruqi M.H., Gim J., Kim S., Song J., Kim J. A layered δ-MnO_2 nanoflake cathode with high zinc-storage capacities for eco-friendly battery applications. *Electrochem. Commun.*, 2015, **60**, P. 121–125.

[15] Cui H.J., Huang H.Z., Fu M.L., Yuan B.L., Pearl W. Facile synthesis and catalytic properties of single crystalline β-MnO_2 nanorods. *Catal. Commun.*, 2011, **12**, P. 1339–1343.

[16] Kumar H., Sangwan M., Sangwan P. Synthesis and characterization of MnO_2 nanoparticles using co-precipitation technique. *Int. J. Chem. Chem. Eng.*, 2013, **3**, P. 155–160.

[17] Samantha Prabath Ratnayake, Jiawen Ren, Elena Colusso, Massimo Guglielmi, Alessandro Martucci, Enrico Della Gaspera. SILAR deposition of metal oxide nanostructured films. *Small*, 2021, 2101666.

[18] Tolstoy V.P. Successive ionic layer deposition. The use in nanotechnology *Russ. Chem. Rev.*, 2006, **75**, P. 161.

[19] Ragupathy P., Vasan H.N., Munichandraiah N. Synthesis and characterization of nano-MnO_2 for electrochemical supercapacitor studies. *J. Electrochem. Soc.*, 2008, **155**, P. 34–40.
[20] Kodintsev I.A., Martinson K.D., Lobinsky A.A., Popkov V.I. SILD synthesis of the efficient and stable electrocatalyst based on CoO-NiO solid solution toward hydrogen production. *Nanosystems: Physics, Chemistry, Mathematics*, 2019, **10** (6), P. 681–685.
[21] Kodintsev I.A., Martinson K.D., Lobinsky A.A., Popkov V.I. Successive ionic layer deposition of co-doped $Cu(OH)_2$ nanorods as electrode material for electrocatalytic reforming of ethanol. *Nanosystems: Physics, Chemistry, Mathematics*, 2019, **10** (5), P. 573–578.
[22] Lobinsky A.A., Kaneva M.V. Synthesis Ni-doped CuO nanorods via successive ionic layer deposition method and their capacitive performance. *Nanosystems: Physics, Chemistry, Mathematics*, 2020, **11** (5), P. 573–578.
[23] Lobinsky A.A., Kaneva M.V. Layer-by-layer synthesis of Zn-doped MnO_2 nanocrystals as cathode materials for aqueous zinc-ion battery. *Nanosystems: Physics, Chemistry, Mathematics*, 2021, **12** (2), P. 182–187.
[24] Lobinsky A.A., Tenevich M.I. Synthesis 2D nanocrystals of Co-doped manganese oxide as cathode materials of zinc-ion hybrid supercapacitor. *Nanosystems: Physics, Chemistry, Mathematics*, 2022, **13** (5), P. 525–529.
[25] Lobinsky A.A., Kodintsev I.A., Tenevich M.I., Popkov V.I. A novel oxidation–reduction route for the morphology-controlled synthesis of manganese oxide nanocoating as highly effective material for pseudocapacitors. *Coatings*, 2023, **13** (2), 361.
[26] Post J.E., Veblen D.R. Crystal structure determinations of synthetic sodium, magnesium, and potassium birnessite using TEM and the Rietveld method. *American Mineralogist*, 1990, **75**.
[27] Min S., Kim Y. Physicochemical characteristics of the birnessite and todorokite synthesized using various methods. *Minerals*, 2020, **10**, P. 1–17.
[28] Sabri M., King H.J., Gummow R.J., Malherbe F., Hocking R.K. The Oxidation of Peroxide by Disordered Metal Oxides: A Measurement of Thermodynamic Stability "By Proxy". *Chempluschem*, 2018, **83**, P. 620–629.
[29] Post J.E., McKeown D.A., Heaney P.J. Raman spectroscopy study of manganese oxides: Layer structures. *American Mineralogist*, 2021, **106**, P. 351–366.
[30] Julien C., et al. Raman spectra of birnessite manganese dioxides. *Solid State Ion*, 2003, **159**, P. 345–356.

Submitted 5 September 2023; accepted 10 October 2023

Information about the authors:

Artem A. Lobinsky – Ioffe Institute, Saint Petersburg, 194021, Russia; ORCID 0000-0001-5930-2087; lobinsky.a@gmail.com

Maria V. Kaneva – Ioffe Institute, Saint Petersburg, 194021, Russia; ORCID 0000-0003-2816-7059; skt94@bk.ru

Anastasia K. Bachina – Ioffe Institute, Saint Petersburg, 194021, Russia; ORCID 0000-0001-7015-1435; a.k.bachina@yandex.ru

Maxim I. Tenevich – Ioffe Institute, Saint Petersburg, 194021, Russia; ORCID 0000-0003-2003-0672; mtenevich@gmail.com

Conflict of interest: the authors declare no conflict of interest.